

Neuronal Induction of the Immunoproteasome in Huntington's Disease

Miguel Díaz-Hernández,^{1*} Félix Hernández,^{1*} Ester Martín-Aparicio,¹ Pilar Gómez-Ramos,² María A. Morán,² José G. Castaño,³ Isidro Ferrer,⁴ Jesús Avila,¹ and José J. Lucas¹

¹Centro de Biología Molecular "Severo Ochoa", Consejo Superior de Investigaciones Científicas (CSIC), Universidad Autónoma de Madrid (UAM), Cantoblanco, 28049 Madrid, Spain, ²Departamento de Morfología, Facultad de Medicina, UAM, 28029 Madrid, Spain, ³Instituto de Investigaciones Biomédicas "Alberto Sols" CSIC/UAM and Departamento de Bioquímica, Facultad de Medicina, UAM, 28029 Madrid, Spain, and ⁴Institut de Neuropatologia, Servei d'Anatomia Patologica, Hospital Princesps d'Espanya, Hospitalet de Llobregat, 08907 Barcelona, Spain

Huntington's disease (HD) inclusions are stained with anti-ubiquitin and anti-proteasome antibodies. This, together with proteasome activity studies on transfected cells, suggest that an impairment of the ubiquitin–proteasome system (UPS) may be key in HD pathogenesis. To test whether proteasome activity is impaired *in vivo*, we performed enzymatic assays for the three peptidase activities of the proteasome in brain extracts from the HD94 conditional mouse model of HD. We found no inhibition of any of the activities, suggesting that if UPS impairment happens *in vivo*, it is not at the level of the proteasome catalytic core. Intriguingly, the chymotrypsin- and trypsin-like activities increased selectively in the affected and aggregate-containing regions: cortex and striatum. Western blot analysis revealed no difference in total proteasome content whereas an increase in the interferon-inducible subunits of the immunoproteasome, LMP2 and LMP7, was observed. These subunits confer to the proteasome catalytic properties that are optimal for MHC-I peptide presentation. Immunohistochemistry in control mouse brain revealed LMP2 and LMP7 mainly in neurons. Accordingly, their increase in HD94 mice predominantly took place in neurons, and 5% of the ubiquitin-positive cortical aggregates were also LMP2-positive. Ultrastructural analysis of neurons with high level of immunoproteasome subunits revealed signs of neurodegeneration like nuclear indentation or fragmentation and dark cell appearance. The neuronal induction of LMP2 and LMP7 and the associated signs of neurodegeneration were also found in HD postmortem brains. Our results indicate that LMP2 and LMP7 participate in normal neuronal physiology and suggest a role in HD neurodegeneration.

Key words: Huntington's disease; proteasome activity; immunoproteasome inducible subunits: LMP2, LMP7; conditional transgenic mouse model; HD postmortem brain

Introduction

Huntington's disease (HD) is an autosomal dominant neurodegenerative disorder caused by a CAG triplet repeat expansion coding for a poly-glutamine (polyQ) sequence in the N-terminal region of the huntingtin (htt) protein (Huntington's Disease Collaborative Research Group, 1993). Patients suffer from motor dysfunction, cognitive decline, and psychological disturbances over 10–15 years until death, caused by atrophy in the striatum and the cortex (Ambrose et al., 1994).

At least eight other autosomal dominant neurological diseases are also caused by a polyQ expansion mutation in their respective proteins. These triplet-repeat disorders share an interesting commonality; the presence of intraneuronal aggregates containing the expanded polyQ (Ross, 1997; Nakamura et al., 2001). These aggregates have been found to be immunopositive for ubiquitin and for proteasome subunits in HD and SCA-1 brains (DiFiglia et al., 1997; Cummings et al., 1998) and in mouse and cell models of most triplet-repeat disorders (Davies et al., 1997; Chai et al., 1999; Stenoien et al., 1999; Martín-Aparicio et al., 2001).

The 20 S proteasome is a large cylindrical multisubunit multicatalytic proteinase that is involved in the degradation of most cytosolic and nuclear proteins (Ciechanover and Schwartz, 1998; Glickman and Ciechanover, 2002). Covalent attachment of a poly-ubiquitin chain to a protein serves as a substrate targeting and recognition signal for the proteasome (DeMartino and Slaughter, 1999; Voges et al., 1999). Polyubiquitylated proteins cannot be degraded directly by the 20 S proteasome. Rather, their degradation requires the 19 S cap that binds to one or both ends of the 20 S proteasome, unfolds substrate proteins, and induces a conformational opening of the outer rings of the 20 S proteasome (DeMartino and Slaughter, 1999).

Received June 18, 2003; revised Sept. 25, 2003; accepted Oct. 22, 2003.

This work was supported by grants from Comunidad Autónoma de Madrid, Asociación Española de Corea de Huntington (ACHE), Fundación "La Caixa", Spanish Comisión Interministerial de Ciencia y Tecnología, and by an institutional grant from Fundación Ramón Areces. E.M.-A. was the recipient of predoctoral fellowships from ACHÉ and Fundación Ferrer. M.D.-H. is the recipient of a postdoctoral fellowship from Comunidad Autónoma de Madrid. We thank Drs. Luis Antón, Javier Díaz-Nido, and Francisco Wandosell for helpful discussion and comments and Dr. Erich E. Wanker for kindly providing CAG53b antibody. We are also grateful to Carlos Sánchez, *Raquel Cuadros, Cristina Plata, and Elena Langa for technical assistance.

*M.D.-H. and F. H. contributed equally to this work.

Correspondence should be addressed to José J. Lucas, Centro de Biología Molecular "Severo Ochoa", Consejo Superior de Investigaciones Científicas, Universidad Autónoma de Madrid, Facultad de Ciencias, Cantoblanco, 28049 Madrid, Spain. E-mail: jjlucas@cbm.uam.es.

Copyright © 2003 Society for Neuroscience 0270-6474/03/2311653-09\$15.00/0

Sequestration of ubiquitylated proteins and of proteasome subunits into polyQ-containing aggregates led to the hypothesis that the activity of the ubiquitin-proteasome system (UPS) might be impaired in CAG triplet-repeat disorders, thus resulting in abnormal neuronal physiology and viability caused by altered turnover of regulatory proteins by the proteasome. Evidence supporting this hypothesis has been obtained in experiments performed on transfected cells (Bence et al., 2001; Jana et al., 2001). Additionally, we have previously reported that aggregates are dynamic structures that are cleared *in vivo* after shut down of mutant-htt expression (Yamamoto et al., 2000) and that this clearance is proteasomal-dependent (Martin-Aparicio et al., 2001).

It is still not known the mechanism by which expanded polyQ inhibits the UPS. This could be by saturating the capacity of one or more chaperones required for UPS function (Bercovich et al., 1997) or by direct interaction with the proteasome either at the level of the catalytic core or at the level of recognition and unfolding for presentation to the catalytic core.

To test whether the catalytic activity of the proteasome is inhibited *in vivo*, we performed assays for the three peptidase activities of the proteasome in HD94 mice. We found no inhibition of any of the activities, thus ruling out a direct effect of the aggregates on the 20 S proteasome. Conversely, we found an increase in chymotrypsin- and trypsin-like activities that can be explained by the also found neuronal increase of the inducible subunits of the proteasome, LMP2 and LMP7. These subunits are selectively induced in antigen-presenting cells, and the resulting proteasomes exhibit altered catalytic characteristics that are optimal to generate peptides for MHC-I antigen presentation (Fruh et al., 1994). The here reported expression and induction of LMP2 and LMP7 in neurons may offer new relevant clues to the role of the proteasome in neuronal physiology and HD pathogenesis.

Materials and Methods

Animals

HD94 mice were generated as previously described (Yamamoto et al., 2000). Mice were bred at the Centro de Biología Molecular "Severo Ochoa" (Madrid, Spain). Four to five mice were housed per cage with food and water available *ad libitum*. Mice were maintained in a temperature-controlled environment on a 12 hr light/dark cycle with light onset at 7:00 A.M.

Antibodies

The following antibodies were used: anti-huntingtin N-terminal CAG53b (amino acids 1–118 with 51 polyglutamines, a kind gift from Dr. Wanker, Berlin, Germany), anti- α -tubulin (Sigma, St. Louis, MO), anti- α -galactosidase (Promega, Madison, WI), anti-ubiquitin (Dako, Carpinteria, CA), anti-poly-ubiquitylated conjugates (FK-2) (Affinity BioReagents, Golden, CO), monoclonal antibodies against 20 S proteasome inducible β subunits: LMP2 (clone LMP2–13), LMP7 (clone LMP7–1), polyclonal antibodies against 20 S proteasome β subunits: LMP2 (PW8205), LMP7 (PW8200), MECL1 (PW8150), β 2/MECL1 (PW8210), polyclonal antibody against 20 S proteasome subunits α 1– α 7 (PW8195), monoclonal antibody against 20 S proteasome subunits β 1 (PW 8140), polyclonal antibody against 20 S proteasome subunits β 5 (PW 8895), and polyclonal antibodies against human 20 S proteasome subunits LMP2 (PW8345), LMP7 (PW8355), and MECL1 (PW8350) (all commercial anti-proteasome subunit antibodies were from Affinity). We also used the fully characterized anti-proteasome polyclonal antibodies raised against the proteasome multicatalytic protease (MPC) (Mengual et al., 1996; Lafarga et al., 2002) and against the COOH-terminal region of C2 subunit (Arribas et al., 1994; Lafarga et al., 2002).

Human samples

Brain specimens used in this study were removed at autopsy from three HD (one woman aged 65 years and two men aged 71 and 68 years) and

three age-matched controls (one woman aged 80 years and two men aged 63 and 79 years) following the protocols of nervous tissue donation approved by the local Ethical Committees of the Barcelona and Bellvitge brain banks. The postmortem delay in tissue processing was between 4 and 15 hr in both groups. The neuropathological examination in HD cases revealed a diagnosis of HD grade 4 following the criteria of Vonsattel et al. (1985), revised in Vonsattel and DiFiglia (1998).

Proteasome activity assays

Brain structures were placed on ice and homogenized in extraction buffer (10 mM Tris-HCl, pH 7.8, 0.5 mM dithiothreitol, 5 mM ATP, 0.03% Triton X-100, and 5 mM MgCl₂). The lysates were centrifuged at 13,000 \times g at 4°C for 20 min. The resulting supernatants were placed on ice and assayed for protein concentrations by the Bradford's method (Bio-Rad, Hercules, CA). For determination of proteasome activity, extracts were adjusted to 0.5 mg/ml total protein by dilution with extraction buffer. All assays were done in triplicate. Chymotrypsin-like activity was determined using the substrate Suc-LLVY-aminomethylcoumarin (AMC) (Sigma; 50 μ M), trypsin-like activity was determined using the substrate Boc-LSTR-AMC (Sigma; 50 μ M), and post-glutamyl activity was determined using the substrate Z-LLE- β -2-naphthylamine (Nap) (Sigma; 0.2 mM). Assay mixtures containing 2 μ g of protein, substrate, and 50 mM HEPES-KOH, pH 7.5, are made up in a final volume of 100 μ l. Incubations were performed at 37°C for 15 and 30 min. The cleavage products AMC and Nap were analyzed, after stopping the reaction with 1 ml of 10% SDS in a fluorimeter (excitation/emission: 333/410 nm for Nap and 380/460 nm for AMC). Product formation was linear with time (at least for 60 min) and with protein concentration up to 4 μ g of protein. Background activity (caused by nonproteasomal degradation) was determined by addition of the proteasome inhibitor lactacystin at a final concentration of 50 μ M (Calbiochem, La Jolla, CA). To ensure maximal content of aggregates, all proteasome activity experiments were performed in aged HD94 mice (at least 1 year old) and age-matched control mice.

Immunohistochemistry

Mouse brain. Mice were anesthetized with a xylazine-ketamine solution and transcardially perfused with 4% paraformaldehyde (PFA) in Sorensen's buffer for 10 min. Brains were postfixed in 4% PFA for 2 hr at 4°C and cryoprotected in 30% sucrose solution. Thirty micrometer sagittal sections were cut on a freezing microtome (Leica, Nussloch, Germany) and collected in 0.1% azide-PBS solution. Next, brain sections were pre-treated for 1 hr with 1% BSA, 5% FBS, and 0.2% Triton X-100 and then incubated with primary antibodies at the following dilutions: monoclonal anti-LMP2 (1:100), polyclonal LMP2 (1:1000), monoclonal anti-LMP7 (1:100), polyclonal LMP7 (1:1000), monoclonal anti-MECL1 (1:100), and anti-ubiquitin (1:500). Finally, brain sections were incubated in avidin-biotin complex using the Elite Vectastain kit (Vector Laboratories, Burlingame, CA). Chromogen reactions were performed with diaminobenzidine (DAB; Sigma) and 0.003% H₂O₂ for 10 min. Sections were coverslipped with Fluorosave.

Human brain. Samples (2-mm-thick) of the frontal cortex and striatum that from control and HD subjects were fixed at the time of the autopsy in 4% paraformaldehyde for 24–48 hr, and then immersed in 30% buffered saccharose for 48 hr. Once cryoprotected, the samples were frozen and stored at –80°C until use. Then, 30 μ m sections were obtained with a cryostat and processed for free-floating immunohistochemistry in the same conditions as described for the mouse samples.

The primary antibodies assayed were the following: monoclonal anti-LMP2 (1:100), polyclonal to human LMP2 (1:1000), monoclonal anti-LMP7 (1:100), and polyclonal to human LMP7 (1:1000). Immunoreaction was visualized with 0.05% DAB and 0.01% H₂O₂ (brown precipitate). Immunohistochemistry plus TUNEL double-labeling was conducted after a two-step protocol. First, the sections were processed for immunohistochemistry, and the peroxidase reaction was visualized with DAB and H₂O₂ (brown precipitate). Then, the sections were processed for the method of *in situ* end-labeling of nuclear DNA fragmentation with ApopTag: *in situ* apoptosis detection kit (Oncor, Gaithersburg, MD) following the instructions of the supplier with some

modifications including omission of proteinase incubation. The reaction was visualized with the nickel protocol (dark blue).

Quantification analysis from immunohistochemistry studies was performed taking images from at least three different sections of independent experiments using Axioskop 2 plus microscope and a CCD camera (Coolsnap FX color). Positive signal was considered for the different antibodies if the mean intensity value was >100 on a 0–255 scale with 0 = black and 255 = white. The cutoff value of 100 was determined from visual analysis of immunolabeling and by comparison with control (maximal level obtained with pre-absorbed antibodies).

Immunofluorescence studies

Sagittal mouse brain sections were pretreated with NH_4Cl 50 mM, 1 M glycine, 1% BSA, and 1% Triton X-100 in PBS buffer and incubated with primary antibodies at the following dilutions: polyclonal anti-LMP2 (1:1000) and monoclonal anti-ubiquitinated conjugates (FK2) (1:10,000). Subsequently, the brain sections were washed with PBS buffer and incubated with secondary antibodies at the following dilutions: goat anti-rabbit IgG labeled with Texas Red from Molecular Probes (Eugene, OR) (1:400) and goat anti-mouse IgG labeled with Oregon Green 488 from Molecular Probes (1:200). Finally, the brain sections were washed with PBS and mounted following the standard procedures. Controls were performed by following the same procedure but substituting the primary antibodies by PBS in presence of 1% BSA.

Colocalization of two markers was analyzed by taking successive Oregon green 488 and Texas Red fluorescent images using an Axioskop 2 plus microscope and a CCD camera (Coolsnap FX color). Positive signal was considered for the different antibodies if the mean intensity value was >140 on a 0–255 scale with 0 = white and 255 = black. The cutoff value of 140 was determined from visual analysis of immunolabeling and by comparison with control (maximal level obtained with preabsorbed antibodies).

Tissue processing for electron microscopy

For electron microscopy, vibratome sections were used. Once immunostained as above described, the sections were postfixed in 2% OsO_4 for 1 hr, dehydrated, embedded in araldite, and flat-mounted in Formvar-coated slides, using plastic coverslips. After polymerization, selected areas were photographed, trimmed, re-embedded in araldite, and resectioned at 1 μm . These semithin sections were re-photographed and resectioned in ultrathin sections. The ultrathin sections were observed in a Jeol electron microscope, without heavy metal staining to avoid artifactual precipitates.

Western blot analysis

Mouse samples. Extracts for Western blot analysis were prepared by homogenizing fresh dissected mouse brain regions in ice-cold extraction buffer consisting of 20 mM HEPES, pH 7.4, 100 mM NaCl, 10 mM NaF, 1% Triton X-100, 1 mM sodium orthovanadate, 10 mM EDTA, and protease inhibitors (2 mM PMSF, 10 $\mu\text{g}/\text{ml}$ aprotinin, 10 $\mu\text{g}/\text{ml}$ leupeptin, and 10 $\mu\text{g}/\text{ml}$ pepstatin). The samples were homogenized at 4°C, and protein content was determined by Bradford assay. Total protein (20 μg) was electrophoresed on 10% SDS-PAGE gel and transferred to a nitrocellulose membrane (Schleicher & Schuell, Keene, NH). The experiments were performed using the following primary antibodies: anti-whole proteasome (MCP, 1:1000), anti-C2-c-terminal (1:1000), anti- α -tubulin (1:20,000), monoclonal anti-LMP2 (1:500), monoclonal anti-LMP7 (1:500), polyclonal anti-LMP7 (1:10,000), monoclonal anti-MECL1 (1:500), polyclonal anti- $\beta 5$ (1:500), and monoclonal anti- $\beta 1$ (1:500). The filters were incubated with the antibody at 4°C overnight in 5% nonfat dried milk. A secondary goat anti-mouse (monoclonal antibodies) or goat anti-rabbit (polyclonal antibodies) antibody (both 1:5000; Invitrogen, Gaithersburg, MD) was used followed by ECL detection (Amersham, Arlington Heights, IL).

Human samples. Fresh samples of the frontal cortex and striatum were obtained at the time of the autopsy, and they were immediately frozen on dry ice and stored at -80°C for biochemical studies. Control and HD brain samples were processed following the same protocol as described for mouse samples.

Quantification of immunoreactivity was performed by using a GS-710

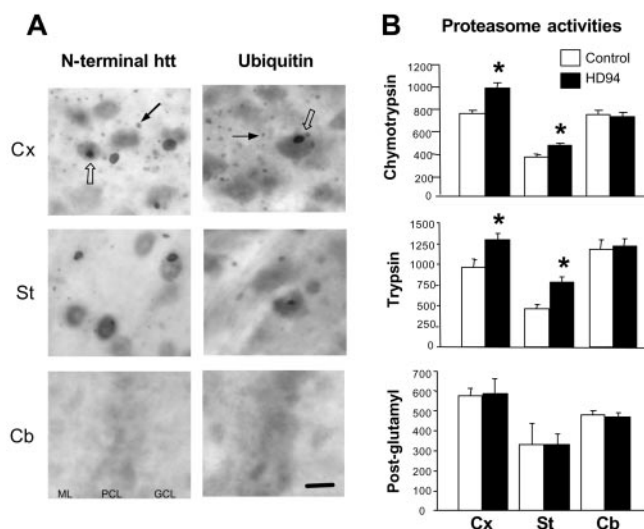


Figure 1. Increased chymotrypsin-like and trypsin-like proteasome activities in aggregate containing brain regions of the HD94 mice. *A*, Immunohistochemistry with anti-N-terminal htt (CAG53b) or anti-ubiquitin antibodies revealed the presence of aggregates in the cortex and the striatum, but not in the cerebellum, of HD94 mice. Both nuclear (empty arrows) and neuropil aggregates (black arrows) can be detected. Cx, Cortex; St, striatum; Cb, cerebellum; ML, molecular layer; PCL, Purkinje cell layer; GCL, granule cell layer. Scale bar, 20 μm . *B*, The chymotrypsin-like, trypsin-like, and post-glutamyl peptidase activities of the proteasome were assayed in brain extracts of control and HD94 mice by incubating with fluorogenic substrates as described in Materials and Methods. The chymotrypsin-like and trypsin-like activities (shown in arbitrary units) were significantly ($*p < 0.01$) increased in the cortex and striatum of HD94 mice with respect to control littermates.

Calibrated Imaging densitometer scanner controller by Quantity One PC software from Bio-Rad. In all cases, the average intensity value of the pixels in a background selected region was calculated and was subtracted from each pixel in the samples. The densitometry values obtained in the linear range of detection with these antibodies were normalized with respect to the values obtained with an anti- α -tubulin antibody to correct for any deviation in loaded amounts of protein. Statistical analysis was performed using one-way ANOVA followed by Bonferroni test.

Results

Increased chymotrypsin- and trypsin-like proteasome activities in cortex and striatum of HD94 mice

HD94 mice express exon 1 htt with a 94 polyQ repeat in the forebrain (under control of the CamKII α promoter) in a tetracycline regulated manner (Yamamoto et al., 2000). As previously shown, HD94 mice develop intraneuronal aggregates that can be detected in cortex and striatum with anti N-terminal (e.g., CAG53b) and anti-ubiquitin antibodies (Yamamoto et al., 2000; Martin-Aparicio et al., 2001) (Fig. 1*A*). To test whether the presence of intraneuronal aggregates results in impaired proteasomal activity *in vivo*, we assayed the chymotrypsin-like, the trypsin-like, and the post-glutamyl peptidase activities of the proteasome in cortical and striatal homogenates from HD94 mice and from control littermates (Fig. 1*B*). The proteasome activities were also assayed in cerebellum as a control brain region devoid of aggregates (Fig. 1*A*). On the contrary to what was expected, we found significantly increased chymotrypsin- and trypsin-like proteasome activities in the cortex and striatum of HD94 mice, whereas no differences were found in the cerebellum. In the case of the post-glutamyl activity, no difference was found between HD94 and control mice in any of the analyzed brain regions (Fig. 1*B*).

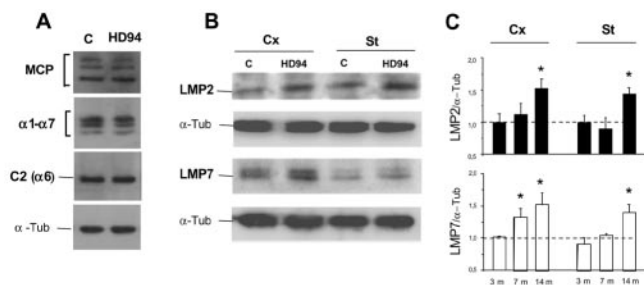


Figure 2. Increased levels of the interferon-inducible subunits of the immunoproteasomes LMP2 and LMP7 in cortex and striatum of HD94 mice. *A*, Western blot analysis of brain cortical extracts of HD94 mice (HD94) and control littermates (C) with the MCP antibody (raised against native 20 S proteasome), the α 1- α 7 antibody (that recognizes six of the seven α -subunits of the 20 S proteasome), and the C2 (α 6) antibody (raised against the C2 COOH-terminal region and that is able to discriminate the active and latent forms of the proteasome). Membranes are probed with an anti-tubulin antibody to correct for any possible deviation on protein loading. *B*, Western blot analysis of brain cortical (Cx) and striatal (St) extracts from 14-month-old HD94 mice and control littermates with antibodies against the LMP2 and LMP7 inducible subunits of the immunoproteasome. Membranes are probed with an anti-tubulin antibody to correct for any possible deviation on protein loading. *C*, Histograms showing the densitometric quantification of LMP2 and LMP7 levels in HD94 versus control samples in 3-, 7-, and 14-month-old mice ($*p < 0.01$).

Increased levels of the inducible subunits of the immunoproteasomes LMP2 and LMP7 in HD94 mice

In view of the unexpected increase in two of the proteasome catalytic activities, we reasoned that a possible explanation could be that the UPS is actually impaired in neurons harboring aggregates and that these neurons have a higher content of proteasomes as an attempt to counteract their decreased activity. To test this possibility, we performed Western blot analysis with different anti-proteasome antibodies (Fig. 2). The polyclonal anti-MCP antibody raised against native 20 S proteasome (Mengual et al., 1996) revealed no difference in proteasome content between HD94 and control mice neither in cortex (Fig. 2*A*) nor in the striatum (data not shown). Similar results were obtained with the α 1-7 antibody that recognizes six of the seven α -subunits of the 20 S proteasome. We therefore concluded that the increase in chymotrypsin- and trypsin-like proteasome activities is not attributable to an increase in proteasome steady-state levels, as could have been anticipated by the fact that the post-glutamyl activity did not increase in parallel.

We next explored possible qualitative changes in the proteasome that might account for an increase in some of the catalytic activities. Because truncation of the C2 (α 6) subunit has been shown to result in activation of proteasome catalytic activity (Arribas et al., 1994), we performed Western blot with an affinity-purified antibody directed against the C2 COOH-terminal that is able to discriminate the active and latent forms of the proteasome. These experiments revealed no difference either in the electrophoretic motility or in the level of C2 (Fig. 2*A*).

Another possible explanation for a qualitative change in the proteasome that could account for increased catalytic activity, and more precisely, of the chymotrypsin- and trypsin-like activities, was the upregulation of the inducible β subunits LMP2, LMP7, and MECL-1. These are catalytic β subunits that are upregulated in antigen-presenting cells in response to various stimuli (like IFN γ or TNF- α), and that replace the constitutive β catalytic subunits (β 1, β 2, and β 5) of the proteasomes (Tanaka and Kasahara, 1998; Kloetzel, 2001; Rock et al., 2002). The resulting proteasomes are called immunoproteasomes and display altered catalytic activities (chymotrypsin- and trypsin-like activi-

ties selectively increased) that are optimal for MHC class I epitope processing (Tanaka and Kasahara, 1998; Kloetzel, 2001; Rock et al., 2002). Despite the very low expression of MHC in the brain, consistent with the notion that the brain is an immunologically privileged organ (Xiao and Link, 1998), and the previously reported low levels of subunits LMP2, LMP7, and MECL-1 in brain compared with other tissues (Noda et al., 2000), we decided to analyze by Western blot whether their levels were altered in HD94 mice. As shown in Figure 2*B*, both LMP2 and LMP7 levels were significantly increased in the cortex (52.3 and 43.2%, respectively; $*p < 0.01$) and the striatum (53.1 and 41.1%, respectively; $*p < 0.01$) of 14-month-old HD94 mice, whereas no changes were found in the cerebellum (data not shown). No significant changes were found in the level of MECL-1 in any of the analyzed brain regions (data not shown). We then analyzed if the increase in LMP2 and LMP7 subunits also takes place in the brain of mice younger than those used for the proteasome activity assays. As shown in Figure 2*C*, no change in the level of these subunits was found in 3-month-old mice despite the presence of aggregates (Martin-Aparicio et al., 2001). In 7-month-old mice, only LMP7 levels were found increased (32.9%; $*p < 0.01$) in the cortex but not in the striatum of HD94 mice, despite substantial striatal atrophy (Yamamoto et al., 2000). Induction of immunoproteasome subunits thus seems to happen in the brain of HD94 mice only after marked neuropathology has developed. Western blot analysis with specific anti- β 1 and anti- β 5 subunit antibodies revealed that the increase in LMP2 and LMP7 subunits was not accompanied by a concomitant decrease in the corresponding constitutive β subunits (data not shown).

The induction of the immunoproteasome subunits in HD94 mice takes place in neurons

We next performed immunohistochemistry experiments to investigate the cell types in which the induction of the immunoproteasomal subunits takes place (Fig. 3). Interestingly, staining with the LMP2-13 monoclonal antibody in the brain of control mice revealed that the most prominent LMP2 immunoreactivity was localized in neurons, and this was the case in most analyzed brain regions (Fig. 3*A* shows LMP2 staining in pyramidal neurons of the cortex, for example). This staining was specific because this immunoreactivity was not observed when primary antibody was omitted or when a nonrelevant monoclonal antibody was used. Apart from neuronal cells, some astrocytes could also be detected, particularly in white matter areas (data not shown). In HD94 mouse brains, the increase in LMP2 immunostaining was found also in neurons and most remarkably in cortical pyramidal cells (Fig. 3*B–D*). Despite the fact that increased LMP2 levels were also found in the striatum of HD94 mice by Western blot (Fig. 2), no evident staining of cell bodies was detected in the striatum (data not shown), thus suggesting that the increase in LMP-2 resides in the observed neuropil staining and most likely in corticostriatal projections. Similar results regarding the neuronal pattern and the increased staining in cortical pyramidal neurons were obtained with the LMP7-1 monoclonal anti LMP-7 antibody (Fig. 3*D*) (data not shown).

A subset of ubiquitin-positive aggregates in the brain of HD94 mice contain LMP2

Interestingly, immunohistochemistry with a polyclonal anti-LMP2 antibody (Fig. 3*C*), apart from confirming the neuronal identity of the cells harboring the increase in LMP2, also revealed aggregates in the cortex of HD94 mice similar in shape to those

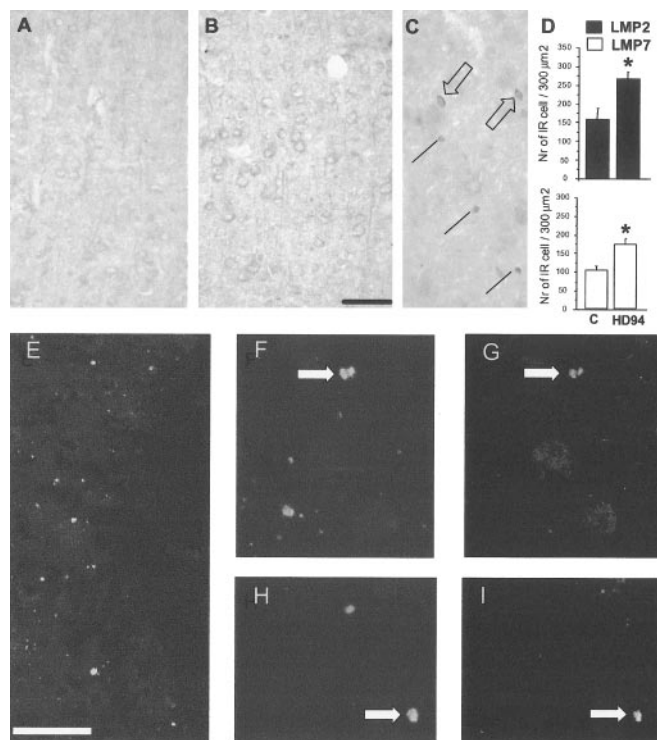


Figure 3. LMP2 is present in neurons and increases in neurons of HD94 mice in which it can be found in ubiquitinated inclusions. Cortical sections from 14-month-old control (*A*), or HD94 mice (*B*, *C*, *E–I*). Cortical pyramidal neurons are revealed by immunohistochemistry with the (LMP2–13) LMP2 monoclonal antibody in control mice (*A*), and this neuronal staining is markedly increased in HD94 mice (*B*, *D*). *C*, The LMP2 polyclonal antibody confirmed the neuronal staining and also revealed LMP2-positive aggregates in the cortex of HD94 mice similar in shape (both ovoid, empty arrows, and spheroid, black arrows) to those detected with anti-ubiquitin antibodies. *D*, Histogram showing the number of LMP2- or LMP7-immunoreactive (IR) cells in the cortex of control and HD94 mice. *E–I*, Double immunofluorescence with anti-polyubiquitin (FK-2 antibody) and LMP2 polyclonal antibodies of HD94 cortical sections. *E* shows the abundance of ubiquitin-positive aggregates in a low-magnification image of the cortex of HD94 mice. White arrowheads in *F–I* show that a subset of ubiquitin-positive aggregates (*F*, *H*) are also LMP2-positive (*G*, *I*). Scale bars: (in *B*) *A*, *B*, 50 μm; *C*, 25 μm; (in *E*), 200 μm; *F–I*, 50 μm.

detected with anti-ubiquitin antibodies (although they were less frequent). We then performed double immunofluorescence studies to determine if LMP2-positive aggregates are a subset of the ubiquitin-positive aggregates or if they are an independent population of inclusions. As shown in Figure 3*E–I*, all LMP2-immunopositive aggregates were also ubiquitin-positive, but they represented only 5% of the total of ubiquitin-positive aggregates.

The induction of LMP2 occurs in degenerating neurons

Immunoelectron microscopy with LMP2 antibodies confirmed the neuronal identity of stained cells in the cortex of either control (Fig. 4*A*) or HD94 mice (Fig. 4*B,C*). The staining, as previously detected by light microscopy, was mainly diffuse cytoplasmic, but the ultrastructural analysis also revealed scattered immunoreactive patches within the nucleus, cytoplasm, and vacuoles of most labeled neurons.

Interestingly, all cortical neurons that at the ultrastructural level showed features of degeneration such as nuclear indentation (Fig. 4*B*) even close to nuclear fragmentation (Fig. 4*B*) or dark appearance (Fig. 4*C*) showed a positive LMP2 immunolabeling.

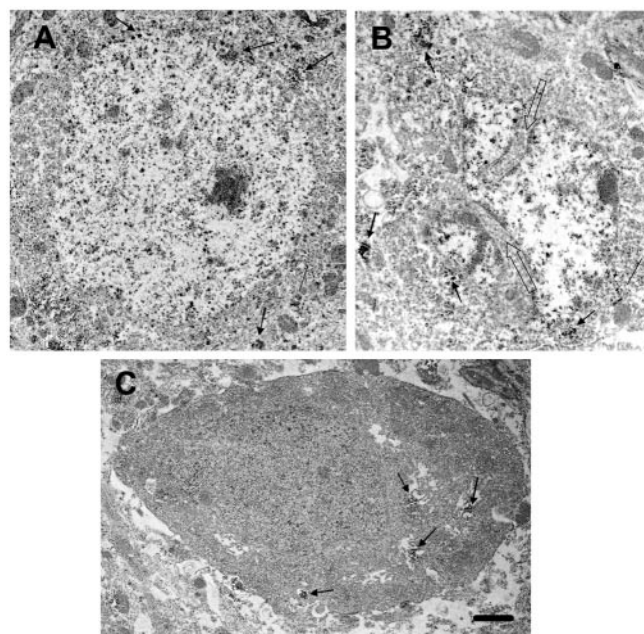


Figure 4. HD94 cortical neurons with heightened levels of LMP2 show signs of neurodegeneration. Immunoelectron microscopy images of control (*A*) or HD94 (*B*, *C*) sections stained with LMP2. *A*, Neuron with cytoplasmic LMP2 staining in the cortex of a control mouse. *B*, Nuclear indentations (empty arrows) in an HD94 cortical LMP2-positive neuron. *C*, LMP2-positive dark neuron in the cortex of an HD94 mouse. Black arrows, Patches of reaction product. Scale bar, 1 μm.

Increased levels of LMP2 and LMP7 in cortex and striatum of HD patients

We then decided to test whether the induction of the immunoproteasome subunits observed in the mouse model of HD also took place in brains of HD patients. We analyzed the level of LMP2 and LMP7 by Western blot in cortex and striatum of grade 4 HD patients and age-matched controls. As shown in Figure 5, the level of LMP2 was 80% higher in the cortex of HD brains than in control brains ($p < 0.01$) and 150% higher in the striatum ($p < 0.01$). Regarding LMP7, the increase was even of higher magnitude both in the cortex (500%; $p < 0.005$) and the striatum (350%; $p < 0.005$) respect to the controls. Western blot analysis with specific anti-β1 and anti-β5 subunit antibodies revealed that the increase in LMP2 and LMP7 subunits was accompanied by a concomitant decrease in the corresponding constitutive β subunits in the striatum ($76.6 \pm 6.5\%$, $p < 0.01$ in the case of the β1 subunit and $56.3 \pm 2.5\%$, $p < 0.01$ in the case of the β5 subunit). However, no change was found in the cortex regarding the level of these constitutive β subunits.

The induction of the immunoproteasome in HD brains also takes place in degenerating neurons

Immunohistochemistry in the cortex of human control subjects and of HD patients with anti-LMP2 (Fig. 6*A,B*) and anti-LMP7 (Fig. 6*C,D*) antibodies yielded very similar results to those found in the mouse model. The neuronal pattern in control samples was even more evident in the human cortex both with LMP2 (Fig. 6*A*) and LMP7 (Fig. 6*C*) antibodies. There was also a marked increase in LMP2 and LMP7 immunoreactivity in cortical neurons of HD brains and, in good agreement with the Western blot data, the increase respect to the control samples was higher than the one found in the mouse model (Fig. 6*B,D,I*).

In the striatum of HD patients, on the contrary to what was described before regarding the mouse model, some LMP2-

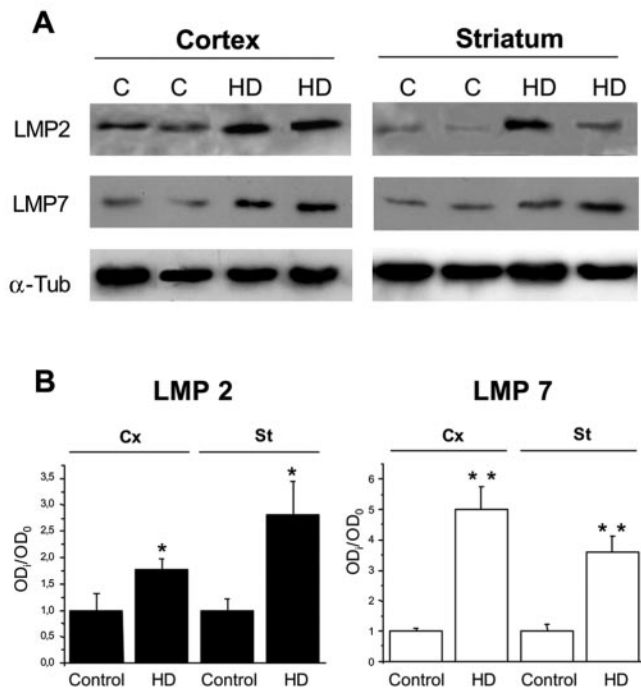


Figure 5. Increased levels of LMP2 and LMP7 in cortex and striatum of HD patients. *A*, Protein extracts were prepared from cortical and striatal postmortem samples of control and HD cases, resolved by SDS-PAGE, and immunoblotted with anti-LMP2, anti-LMP7, and anti- α -tubulin antibodies. *B*, Histograms showing the densitometric quantification of the increase in LMP2 and LMP7 in HD versus control samples (* $p < 0.01$; ** $p < 0.005$).

immunoreactive neurons could be found (Fig. 6*G,H*). Interestingly, some of these neurons were also TUNEL-positive (Fig. 6*H*). Regarding LMP7 immunostaining in the human striatum, a faint staining could be detected in the somas of some medium size spiny neurons in control samples (Fig. 6*E*). The intensity and the number of labeled neurons markedly increased in the striatum of HD cases (Fig. 6*F,J*).

Immunoelectron microscopy in the human samples (Fig. 7) once again confirmed the neuronal identity of LMP2- and LMP7-labeled cells. The ultrastructural analysis also revealed that cortical pyramidal neurons of HD cases with increased LMP2 and LMP7 staining present nuclear indentation similar to what was described for the mouse model (Fig. 7*B*) (data not shown).

Discussion

In this study, by performing proteasome activity assays in brain extracts from the HD94 conditional mouse model of HD (that contain polyQ and ubiquitin-positive aggregates), we have found that the 20 S proteasome activity is not decreased when compared with extracts from control mice. On the contrary, two of the proteolytic activities of the proteasome were increased in the extracts from HD94 mice without a change in total proteasome content. These data revealed a qualitative change in HD94 proteasomes that can be explained by an increase in the level of inducible subunits of the immunoproteasomes LMP2 and LMP7. Because we found that this increase mainly takes place in neurons and that those neurons show signs of neurodegeneration, our data suggest a role of the immunoproteasome in normal neurophysiology as well as in HD pathogenesis.

The initial aim of this study was to test if, as suggested by studies on transfected cells (Bence et al., 2001; Jana et al., 2001), the UPS is impaired *in vivo* in a mouse model of HD. The HD94

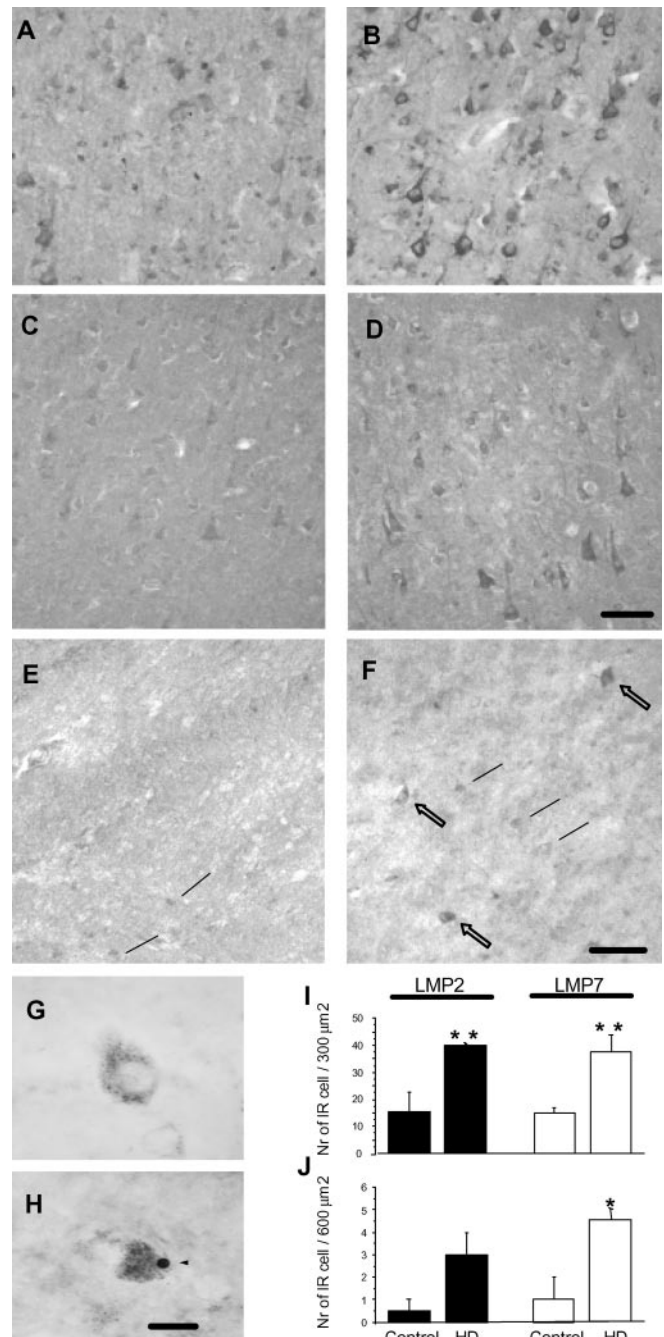


Figure 6. The increase in LMP2 and LMP7 in HD brains takes place in neurons and correlates with TUNEL staining in the striatum. *A–D*, Cortical section from control (*A, C*) or HD brains (*B, D*) stained with anti-LMP2 (*A, B*) or anti-LMP7 (*C, D*) antibodies. *E, F*, LMP7 immunohistochemistry in the striatum of a control (*E*) or HD case (*F*). Arrows indicate medium-size spiny neurons with faint (black arrows) or strong (empty arrows) LMP7 staining. *G*, LMP2-immunostained medium-sized spiny neuron in the striatum of an HD case. *H*, LMP2 and TUNEL double-labeled medium-size spiny neuron in the striatum of an HD case. *I*, Histogram showing the number of LMP2- or LMP7-immunoreactive (IR) cells in the cortex of control and HD brains. *J*, Histogram showing the number of LMP2- or LMP7-immunoreactive cells in the striatum of control and HD brains. Scale bars: (in *D*) *A–D*, 40 μ m; (in *F*) *E, F*, 50 μ m; (in *H*) *G, H*, 10 μ m.

mice we used here (Yamamoto et al., 2000) express exon 1 mutant huntingtin under control of the CamKII α promoter (that drives expression to forebrain neurons) leading to aggregate formation in cortical and striatal neurons (the brain areas affected in HD). If we had gotten the expected result of decreased 20 S pro-

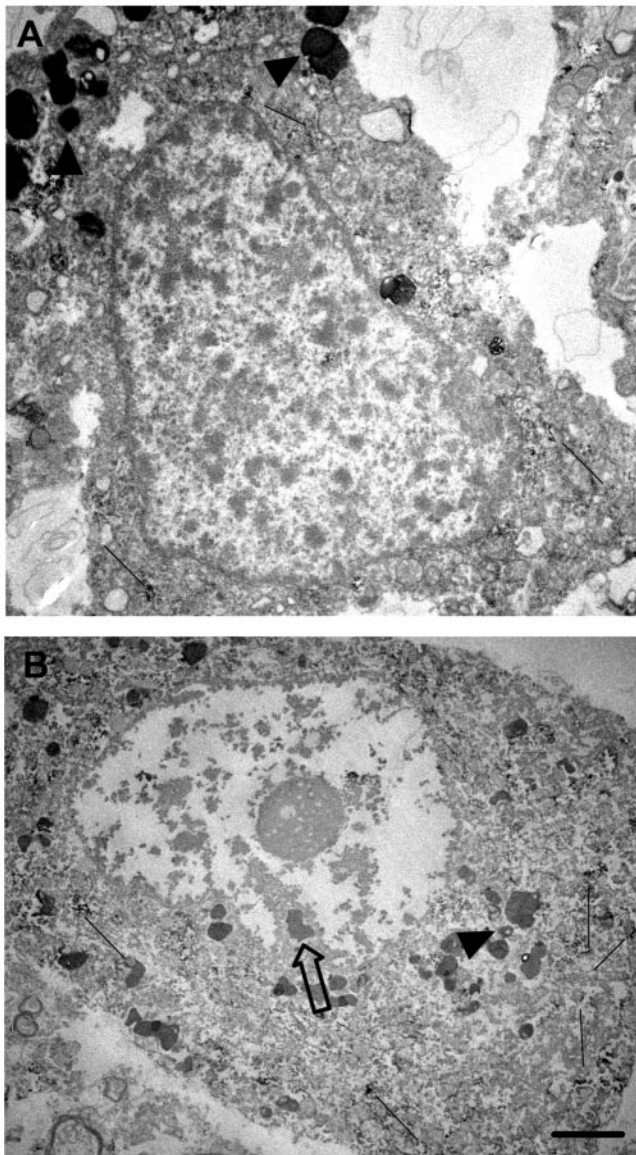


Figure 7. Ultrastructural analysis of LMP7-positive neurons from the cortex of HD patients. Immunoelectronmicroscopy images of cortical section from control (*A*) or HD human samples (*B*) stained with LMP7. *A*, Neuron with cytoplasmic LMP7 staining in the cortex of control subject. *B*, Nuclear indentations (empty arrows) in LMP7-positive cortical neurons from HD cases. Black arrows, Patches of reaction product. Arrowheads, Lipofuscin accumulations. Scale bar, 1 μ m.

teasome peptidase activity in the aggregate-containing brain extracts, we would have assumed that an impairment of the UPS occurs *in vivo* in the aggregate-containing neurons of the mouse model. However, we did not detect decreased proteasome activity in the cell extracts (in fact we got the opposite result in the case of the chymotrypsin- and trypsin-like activities and no change in the case of the post-glutamyl activity). Therefore, our results strongly suggest that the proteasome peptidase activity is not inhibited in the neurons of the HD94 mice by the presence of aggregates. However, because we are measuring total proteasome activities not only for aggregate-containing neurons, but also in non-aggregate-containing neurons and other cell types such as glia, the possibility still exists that proteasome activity is decreased in some aggregate-containing neurons and that more numerous neurons without aggregates and/or glial cells have in-

creased proteasome activity, averaging a final increased proteasome activity for the whole cellular population.

Our data, despite suggesting that a decrease in 20 S proteasome activity does not happen in HD94 neurons, cannot rule out that impairment of the UPS does take place in the brain of HD94 mice at a level different than 20 S proteasome intrinsic catalytic activity. The reason for this is that small fluorogenic substrates are degraded by the 20 S proteasome in a ubiquitination-independent manner. Therefore, these assays can detect alterations in the catalytic activity of the 20 S proteasome, but will fail to detect, alterations at any other level of the UPS such as availability of free ubiquitin, polyubiquitination, recognition by the 19S proteasome, and/or unfolding and presentation to the 20 S proteasomes.

Therefore, to elucidate whether the UPS is impaired *in vivo*, a different approach will be required (Hernández et al., 2004). Such an approach could be the generation of mice with neuronal expression of a reporter protein with a tag for efficient degradation by the UPS (like the GFPu used in the cell transfection experiments (Bence et al., 2001)). We are currently generating this type of mice. Interestingly, very recently, UPS reporter mice have been generated that express a different type of UPS reporter substrate (Ub-G76V-GFP) (Lindsten et al., 2003).

There is a discrepancy between the studies reporting decreased proteasome activity with fluorogenic substrates in transfected (Bence et al., 2001; Jana et al., 2001) or infected (Nishitoh et al., 2002) cells that express expanded polyQ-containing proteins, and our data from the mouse model. The most plausible explanation for this is that the level of expression of the pathogenic protein within the transfected or infected cell is much higher than in the transgenic tissue. The level of expression obtained in the transgenic tissue is supposed to be less artifactual because it is high enough to elicit neuronal neuropathology and symptomatology in adult mice, but low enough not to cause premature and artifactual death of the neurons expressing the pathogenic protein. Because we have performed the studies on aggregate-containing extracts from symptomatic mice, our data probably reflect better the situation in the affected neurons in an HD patient. In this regard, there is another report of transfected cells expressing GFP with expanded polyQ sequences, in which no inhibition of proteasome activity could be detected with fluorogenic substrates (Ding et al., 2002). Interestingly, this study was performed in stably transfected SH-SY5Y cells that probably elicit lower levels of expression of the foreign protein (as evidenced by the lack of aggregate formation) in comparison to the conditionally overexpressing N2A Tet-Off transfected cells (Jana et al., 2001) or the infected primary neurons (Nishitoh et al., 2002).

Regarding the mechanism by which expression of mutant htt results in increased levels of LMP2 and LMP7, it is possible that the UPS could actually be impaired *in vivo* in the HD94 mice and that the induction of the immunoproteasome subunits would be a compensatory action of the affected neurons trying to counteract the decreased clearance of proteins. Other possibilities regarding the mechanism by which expression of mutant htt results in increased levels of LMP2 and LMP7 are: (1) that these genes (located in the MHC genome region and that usually show a parallel transcriptional regulation (Beck and Trowsdale, 1999)) are part of the alterations in gene transcription elicited by the expression of toxic polyQ-containing proteins. If this is the case, an increase in LMP2 and LMP7 would be expected in other CAG triplet repeat disorders, (2) that neurons produce LMP2 and LMP7 expression in response to proinflammatory cytokines

(such as IFN γ) released by reactive glia, similarly to what happens in lymphocytes and other antigen-presenting cells. In this regard, we have previously shown that HD94 mice have reactive gliosis in striatum and cortex (Yamamoto et al., 2000) and we have shown here the expression of LMP2 by satellite glia adjacent to LMP2-positive neurons. If the induction of LMP2 and LMP7 were secondary to neuroinflammation, as a corollary, it would be expected to happen also in another neurodegenerative diseases with a marked reactive gliosis such as Alzheimer's disease (Akiyama et al., 2000) and in related animal models with a strong gliosis (Lucas et al., 2001; Hernández et al., 2002). We are currently exploring these possibilities.

The correlation between heightened levels of LMP2 and LMP7 and signs of neurodegeneration suggests that the induction of the immunoproteasome might have pathogenic implications. However, it is also possible that the neurodegeneration is secondary to neuroinflammatory stress, and the induction of the immunoproteasome subunits could just be a marker of neurons degenerating by this mechanism. This is supported by the observation that LMP2 and LMP7 induction takes place only after substantial neuropathology has developed in HD94 brains and by the fact that decreased level of constitutive β 1 and β 5 subunits is observed only in the striatum (the most affected region) of grade 4 HD human brains. In any case, it cannot be ruled out that altered proteolytic processing of proteasome substrates (because of the altered proteolytic activities) might also contribute to the toxicity elicited by expanded polyQ in advanced stages of the disease.

Regarding the possible implications of the induction of the interferon-inducible subunits of the immunoproteasome, because these confer to the proteasomes catalytic properties that are optimal to generate peptides for MHC-I antigen presentation, it would be interesting to explore if the levels of MHC-I molecules are also altered in HD. Many of the genes participating in MHC-I antigen presentation are located within the MHC genome region and show parallel transcriptional regulation (Beck and Trowsdale, 1999). Furthermore, it has been suggested that MHC-I may participate in neuronal plasticity (Boulanger et al., 2001), and neuronal induction of MHC-I has been shown to happen only in electrically silent neurons, thus suggesting a possible implication in immunosurveillance on functionally impaired neurons (Neumann et al., 1995).

In summary, the data presented here, apart from revealing a role of the immunoproteasome in normal neuronal physiology, bring new light on the status of the UPS *in vivo* in HD and offer new clues about the intraneuronal changes that may contribute to the neuronal dysfunction and eventual neuronal death that are responsible for HD symptomatology.

References

- Akiyama H, Barger S, Barnum S, Bradt B, Bauer J, Cole GM, Cooper NR, Eikelenboom P, Emmerling M, Fiebich BL, Finch CE, Frautschy S, Griffin WS, Hampel H, Hull M, Landreth G, Lue L, Mrak R, Mackenzie IR, McGeer PL, et al. (2000) Inflammation and Alzheimer's disease. *Neurobiol Aging* 21:383–421.
- Ambrose CM, Duyao MP, Barnes G, Bates GP, Lin CS, Srinidhi J, Baxendale S, Hummerich H, Lehrach H, Altherr M, Wasmuth J, Buckler A, Church D, Housman D, Berks M, Micklem G, Durbin R, Dodge A, Read A, Gusella J, et al. (1994) Structure and expression of the Huntington's disease gene: evidence against simple inactivation due to an expanded CAG repeat. *Somat Cell Mol Genet* 20:27–38.
- Arribas J, Arizti P, Castano JG (1994) Antibodies against the C2 COOH-terminal region discriminate the active and latent forms of the multicatalytic proteinase complex. *J Biol Chem* 269:12858–12864.
- Beck S, Trowsdale J (1999) Sequence organisation of the class II region of the human MHC. *Immunol Rev* 167:201–210.
- Bence NF, Sampat RM, Kopito RR (2001) Impairment of the ubiquitin-proteasome system by protein aggregation. *Science* 292:1552–1555.
- Bercovich B, Stancovski I, Mayer A, Blumenfeld N, Laszlo A, Schwartz AL, Ciechanover A (1997) Ubiquitin-dependent degradation of certain protein substrates *in vitro* requires the molecular chaperone Hsc70. *J Biol Chem* 272:9002–9010.
- Boulanger LM, Huh GS, Shatz CJ (2001) Neuronal plasticity and cellular immunity: shared molecular mechanisms. *Curr Opin Neurobiol* 11:568–578.
- Chai Y, Koppenhafer SL, Shoosmith SJ, Perez MK, Paulson HL (1999) Evidence for proteasome involvement in polyglutamine disease: localization to nuclear inclusions in SCA3/MJD and suppression of polyglutamine aggregation *in vitro*. *Hum Mol Genet* 8:673–682.
- Ciechanover A, Schwartz AL (1998) The ubiquitin-proteasome pathway: the complexity and myriad functions of proteins death. *Proc Natl Acad Sci USA* 95:2727–2730.
- Cummings CJ, Mancini MA, Antalffy B, DeFranco DB, Orr HT, Zoghbi HY (1998) Chaperone suppression of aggregation and altered subcellular proteasome localization imply protein misfolding in SCA1. *Nat Genet* 19:148–154.
- Davies SW, Turmaine M, Cozens BA, DiFiglia M, Sharp AH, Ross CA, Scherzinger E, Wanker EE, Mangiarini L, Bates GP (1997) Formation of neuronal intranuclear inclusions underlies the neurological dysfunction in mice transgenic for the HD mutation. *Cell* 90:537–548.
- DeMartino GN, Slaughter CA (1999) The proteasome, a novel protease regulated by multiple mechanisms. *J Biol Chem* 274:22123–22126.
- DiFiglia M, Sapp E, Chase K, Davies S, Bates G, Vonsattel J, Aronin N (1997) Aggregation of huntingtin in neuronal intranuclear inclusions and dystrophic neurites in brain. *Science* 277:1990–1993.
- Ding Q, Lewis JJ, Strum KM, Dimayuga E, Bruce-Keller AJ, Dunn JC, Keller JN (2002) Polyglutamine expansion, protein aggregation, proteasome activity, and neural survival. *J Biol Chem* 277:13935–13942.
- Fruh K, Gossen M, Wang K, Bujard H, Peterson PA, Yang Y (1994) Displacement of housekeeping proteasome subunits by MHC-encoded LMPs: a newly discovered mechanism for modulating the multicatalytic proteinase complex. *EMBO J* 13:3236–3244.
- Glickman MH, Ciechanover A (2002) The ubiquitin-proteasome proteolytic pathway: destruction for the sake of construction. *Physiol Rev* 82:373–428.
- Huntington's Disease Collaborative Research Group (1993) A novel gene containing a trinucleotide repeat that is expanded and unstable on Huntington's disease chromosomes. *Cell* 72:971–983.
- Hernández F, Borrell J, Guaza C, Avila J, Lucas JJ (2002) Spatial learning deficit in transgenic mice that conditionally overexpress GSK-3 β in the brain but do not form tau filaments. *J Neurochem* 83:1529–1533.
- Hernández F, Díaz-Hernández M, Avila J, Lucas JJ (2004) Testing the ubiquitin-proteasome hypothesis of neurodegeneration. *Trends Neurosci*, in press.
- Jana NR, Zemskov EA, Wang G, Nukina N (2001) Altered proteasomal function due to the expression of polyglutamine-expanded truncated N-terminal huntingtin induces apoptosis by caspase activation through mitochondrial cytochrome c release. *Hum Mol Genet* 10:1049–1059.
- Kloetzel PM (2001) Antigen processing by the proteasome. *Nat Rev Mol Cell Biol* 2:179–187.
- Lafarga M, Fernandez R, Mayo I, Berciano MT, Castano JG (2002) Proteasome dynamics during cell cycle in rat Schwann cells. *Glia* 38:313–328.
- Lindsten K, Menendez-Benito V, Masucci MG, Dantuma NP (2003) A transgenic mouse model of the ubiquitin/proteasome system. *Nat Biotechnol* 21:897–902.
- Lucas JJ, Hernández F, Gomez-Ramos P, Moran MA, Hen R, Avila J (2001) Decreased nuclear beta-catenin, tau hyperphosphorylation and neurodegeneration in GSK-3 β conditional transgenic mice. *EMBO J* 20:27–39.
- Martin-Aparicio E, Yamamoto A, Hernández F, Hen R, Avila J, Lucas JJ (2001) Proteasomal-dependent aggregate reversal and absence of cell death in a conditional mouse model of Huntington's disease. *J Neurosci* 21:8772–8781.
- Mengual E, Arizti P, Rodrigo J, Gimenez-Amaya JM, Castano JG (1996) Immunohistochemical distribution and electron microscopic subcellular localization of the proteasome in the rat CNS. *J Neurosci* 16:6331–6341.
- Nakamura K, Jeong SY, Uchihara T, Anno M, Nagashima K, Nagashima T,

- Ikeda S, Tsuji S, Kanazawa I (2001) SCA17, a novel autosomal dominant cerebellar ataxia caused by an expanded polyglutamine in TATA-binding protein. *Hum Mol Genet* 10:1441–1448.
- Neumann H, Cavalie A, Jenne DE, Wekerle H (1995) Induction of MHC class I genes in neurons. *Science* 269:549–552.
- Nishitoh H, Matsuzawa A, Tobiume K, Saegusa K, Takeda K, Inoue K, Hori S, Kakizuka A, Ichijo H (2002) ASK1 is essential for endoplasmic reticulum stress-induced neuronal cell death triggered by expanded polyglutamine repeats. *Genes Dev* 16:1345–1355.
- Noda C, Tanahashi N, Shimbara N, Hendil KB, Tanaka K (2000) Tissue distribution of constitutive proteasomes, immunoproteasomes, and PA28 in rats. *Biochem Biophys Res Commun* 277:348–354.
- Rock KL, York IA, Saric T, Goldberg AL (2002) Protein degradation and the generation of MHC class I-presented peptides. *Adv Immunol* 80:1–70.
- Ross CA (1997) Intranuclear neuronal inclusions: a common pathogenic mechanism for glutamine-repeat neurodegenerative diseases? *Neuron* 19:1147–1150.
- Stenoien DL, Cummings CJ, Adams HP, Mancini MG, Patel K, DeMartino GN, Marcelli M, Weigel NL, Mancini MA (1999) Polyglutamine-expanded androgen receptors form aggregates that sequester heat shock proteins, proteasome components and SRC-1, and are suppressed by the HDJ-2 chaperone. *Hum Mol Genet* 8:731–741.
- Tanaka K, Kasahara M (1998) The MHC class I ligand-generating system: roles of immunoproteasomes and the interferon-gamma-inducible proteasome activator PA28. *Immunol Rev* 163:161–176.
- Voges D, Zwickl P, Baumeister W (1999) The 26S proteasome: a molecular machine designed for controlled proteolysis. *Annu Rev Biochem* 68:1015–1068.
- Vonsattel JP, DiFiglia M (1998) Huntington disease. *J Neuropathol Exp Neurol* 57:369–384.
- Vonsattel JP, Myers RH, Stevens TJ, Ferrante RJ, Bird ED, Richardson EP Jr (1985) Neuropathological classification of Huntington's disease. *J Neuropathol Exp Neurol* 44:559–577.
- Xiao BG, Link H (1998) Immune regulation within the central nervous system. *J Neurol Sci* 157:1–12.
- Yamamoto A, Lucas JJ, Hen R (2000) Reversal of neuropathology and motor dysfunction in a conditional model of Huntington's disease. *Cell* 101:57–66.